Evolution of two-dimensional lump nanosolitons for the Zakharov-Kuznetsov and electromigration equations

M. C. Jorge[a] and Gustavo Cruz-Pacheco[b]
FENOMEC, Department of Mathematics and Mechanics, I.I.M.A.S., Universidad Nacional Autónoma de Mexico, Apdo. 20-726, 01000 México, D.F.

Luis Mier-y-Teran-Romero[c]
Department of Physics, Northwestern University, Evanston, Illinois, 60208

Noel F. Smyth[d]
School of Mathematics, The King's Buildings, University of Edinburgh, Edinburgh, EH9 3JZ Scotland, United Kingdom

(Received 14 October 2004; accepted 2 February 2005; published online 21 October 2005)

The evolution of lump solutions for the Zakharov-Kuznetsov equation and the surface electromigration equation, which describes mass transport along the surface of nanoconductors, is studied. Approximate equations are developed for these equations, these approximate equations including the important effect of the dispersive radiation shed by the lumps as they evolve. The approximate equations show that lumplike initial conditions evolve into lump soliton solutions for both the Zakharov-Kuznetsov equation and the surface electromigration equations. Solutions of the approximate equations, within their range of applicability, are found to be in good agreement with full numerical solutions of the governing equations. The asymptotic and numerical results predict that localized disturbances will always evolve into nanosolitons. Finally, it is found that dispersive radiation plays a more dominant role in the evolution of lumps for the electromigration equations than for the Zakharov-Kuznetsov equation. © *2005 American Institute of Physics*.
[DOI: 10.1063/1.1877892]

The phenomenon of electromigration plays a major role in nanocircuits in electronics as it leads to undesirable surface instabilities. In order to suppress or delay the onset of these instabilities it is necessary to have a quantitative understanding of them. A step in this direction is to model the surface of a conductor as a free surface with appropriate boundary conditions. Under the assumption of unidirectional waves which have small lateral dispersion, it is shown that the instabilities are governed by a Zakharov-Kuznetsov (ZK) type equation for the surface waves, coupled to an elliptic equation for the electrostatic potential. This coupled system of equations is nonintegrable and numerical solutions show that disturbances propagate as lump solitons in two spatial dimensions. Moreover, as a lump propagates, it sheds radiation and it is found that this radiation plays a dominant role in the evolution of the lump. In the present work the evolution of lump disturbances is studied asymptotically and numerically. It is shown by using a combination of an approximate theory (collective coordinates) for the lump evolution, coupled to a geometric optics solution for the shed radiation, how an initial lump evolves by shedding radiation into a traveling, stable, coherent lump structure. It is shown that all initial conditions ultimately evolve into such lumps. This evolution is also studied for higher order nonlinearity and it is shown that, despite the shed radiation, an initial lump collapses in finite time if it has a large enough initial amplitude. Finally, due to the simplicity of the equations and the shed radiation pattern, we are able to extend the theory to the full three space dimensional case. In this full three-dimensional case, similar behavior as in two spatial dimensions is found. The present work therefore suggests that instabilities always form and keep their coherence over long distances. Thus in order to eliminate instabilities in nanocircuits, it is necessary that the surface of the conductor is coupled to a mechanism capable of producing a threshold for the instability, such as a surface coating.

I. INTRODUCTION

In the present work the evolution of coherent structures for the Zakharov-Kuznetsov (ZK) equation will be considered. The ZK equation describes small amplitude, nonlinear waves propagating in two spatial dimensions.[1] The derivation of this equation assumes that the propagation of the waves is fundamentally unidirectional, as for the one space dimensional Korteweg–de Vries (KdV) equation, and that the waves have a relatively weak lateral dispersion. The ZK equation, like the KP equation, is a generalization of the KdV equation to two space dimensions which takes account of weak lateral dispersion.

In previous work the linear stability of the planar KdV soliton, which is a solution of the ZK equation, with respect

[a]Electronic mail: mcj@mym.iimas.unam.mx
[b]Electronic mail: cruz@mym.iimas.unam.mx
[c]Electronic mail: l-mieryt@northwestern.edu
[d]Author to whom correspondence should be addressed. Electronic mail: N.Smyth@ed.ac.uk

to long wave transverse perturbations was studied. It was shown in Refs. 2–4 that for long transverse wave perturbations the KdV soliton is unstable. This instability was followed numerically in Ref. 5 and it was observed that an initially transversely uniform soliton breaks up into several lumplike structures. These structures were identified as cylindrical solitarylike waves.

More recently the ZK equation coupled to a nonlinear Laplace-type equation has been obtained in the study of surface electromigration in nanoconductors subject to strong, unidirectional electric fields.[6,7] In this situation the surface electromigration of electrons deforms the conductor. In the early stages, this deformation can be identified with a ZK lump solitary wave. In many other applications, a ZK-type equation arises, but with a different order nonlinearity,[8] so that the resulting equation is a possible two-dimensional counterpart of the mKdV equation.[9]

In the present work the evolution of an initial condition close to a lump soliton for the ZK equation will be studied. As in previous work for the KP equation,[10] this evolution is studied using an approximate theory, which couples the lump soliton to the dispersive radiation shed as it evolves. The present work considers the general cases of a ZK equation with an arbitrary order nonlinearity and the ZK equation coupled to a potential equation, as arising in electromigration in nanoconductors. It is found that lumplike initial conditions evolve into steadily propagating Gaussian soliton solutions by shedding mass in the form of dispersive radiation. It is further found that, as expected, this shed dispersive radiation plays a critical role in the stabilization of the soliton. A major difference between the ZK equation and the electromigration equations is that the shed radiation has a greater effect on the evolution of the pulse in the case of the electromigration equations, with the radiation carrying a significant amount of momentum. When the nonlinearity in the ZK equation is higher than a quadratic, the approximate equations show that initial conditions with mass below a certain threshold decay, while those with mass above the threshold blow up in finite time. Finally, it is found that there is very good agreement between full numerical solutions of the ZK equation and solutions of the approximate equations, which include the effects of shed radiation.

The paper is organized as follows. In the second section the basic ZK equations in two and three space dimensions are formulated. In the third section, approximate equations for a lump solution of the single ZK equation are derived, these equations also taking account of the dispersive radiation shed as the lump evolves. The fourth section extends the approximate equations for the ZK equation to three space dimensions. In the fifth section, corresponding approximate equations for the ZK system governing electromigration are derived with the sixth section presenting comparisons between full numerical solutions of the governing equations and solutions of the approximate equations. Finally, the last section presents the conclusions.

II. FORMULATION

The ZK equation[1] in nondimensional variables is

$$\frac{\partial u}{\partial t}+6u\frac{\partial u}{\partial x}+\frac{\partial^3 u}{\partial x^3}+\frac{\partial^3 u}{\partial x\partial y^2}=0. \tag{1}$$

This equation is subject to a general initial condition $u(x,y,0)=f(x,y)$. Here x is the coordinate in the direction of propagation of the soliton and y is the direction transverse to this. The amplitude of the disturbance is u and t is the time variable. The last term in the ZK equation (1) accounts for weak lateral dispersion. The modified ZK equation with a general nonlinearity is obtained from the ZK equation by replacing u in the convective term by u^p.

The coupled system of the ZK equation and a potential equation governing electromigration in nanoconductors[7] is

$$\frac{\partial u}{\partial t}+6u\frac{\partial u}{\partial x}+\frac{\partial^3 u}{\partial x^3}+\frac{\partial^3 u}{\partial x\partial y^2}+\frac{1}{2}\left(\frac{\partial u}{\partial x}\frac{\partial \Psi}{\partial x}+\frac{\partial u}{\partial y}\frac{\partial \Psi}{\partial y}\right)=0, \tag{2}$$

$$\frac{\partial^2 \Psi}{\partial x^2}+\frac{\partial^2 \Psi}{\partial y^2}=\frac{\partial u}{\partial x}, \tag{3}$$

together with the initial conditions $u(x,y,0)=f(x,y)$ and $\Psi(x,y,0)=(\nabla^2)^{-1}f_x(x,y)$. In this application the variable u is the surface displacement and Ψ is the electrostatic potential on the surface of the conductor. The ZK equation is then modified by the convective term $\nabla u\cdot\nabla\Psi$. The electrostatic potential Ψ is in turn determined by the motion of the free surface.[6,7]

The ZK equation (1) with a general nonlinearity[8] has a straightforward counterpart in three spatial dimensions

$$\frac{\partial u}{\partial t}+6u^p\frac{\partial u}{\partial x}+\frac{\partial}{\partial x}\left(\frac{\partial^2 u}{\partial x^2}+\frac{\partial^2 u}{\partial y^2}+\frac{\partial^2 u}{\partial z^2}\right)=0, \tag{4}$$

together with the initial condition $u(x,y,z,0)=f(x,y,z)$. The nonlinear power p must be a positive integer since u can be negative.

In the present work the evolution of u for the ZK equations (1) and (4) and the ZK system (2) and (3) will be analyzed for the specific initial conditions

$$f(x,y)=Ae^{-\kappa(x^2+y^2)} \quad \text{and} \quad f(x,y,z)=Ae^{-\kappa(x^2+y^2+z^2)}. \tag{5}$$

Finally, it should be noted that the ZK equations (1), (2), and (4) satisfy the mass conservation equation

$$\frac{d}{dt}\int_{-\infty}^{\infty} u\,dV=0 \tag{6}$$

and the momentum conservation equation

$$\frac{d}{dt}\int_{-\infty}^{\infty} u^2\,dV=0, \tag{7}$$

where dV is appropriately interpreted as $dxdy$ in two dimensions and $dxdydz$ in three dimensions. These conservation equations follow from the ZK equations for u on integrating by parts.

Numerical solutions of the ZK equation (1) for the parameter values $A=0.4$ and $\kappa=0.05$ for the initial condition (5) and the electromigration equations (2) and (3) for the parameter values $A=0.3$ and $\kappa=0.05$ for the same initial con-

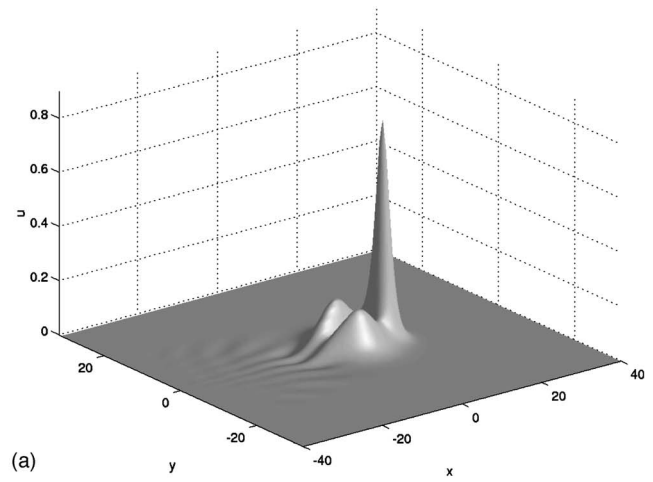

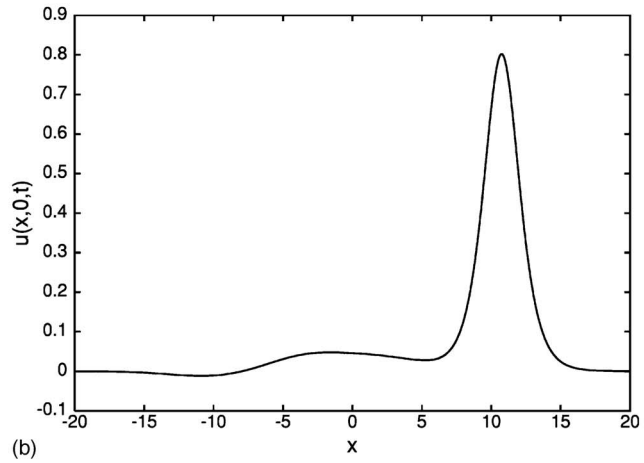

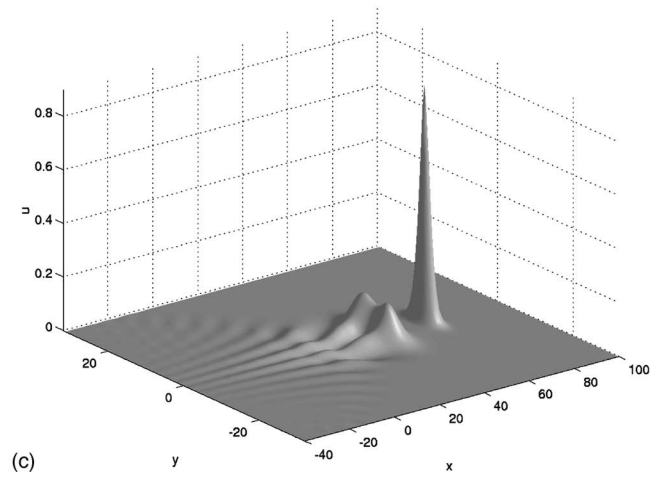

FIG. 1. Numerical solution of the ZK equation (1) for the initial condition (5) with $A=0.4$ and $\kappa=0.05$. (a) Solution at $t=10$. (b) Section of solution along $y=0$ at $t=10$. (c) Solution at $t=25$.

dition are displayed in Figs. 1 and 2. In Fig. 1(a) the numerical solution of the ZK equation (1) at $t=10$ is shown, with a cross section through $y=0$ at this same time shown in Fig. 1(b). A shelf of radiation behind the evolving lump can be clearly seen, although the shelf has a variation in the y direction which will not be accounted for in the present work. Figure 1(c) shows the numerical solution of the ZK equation

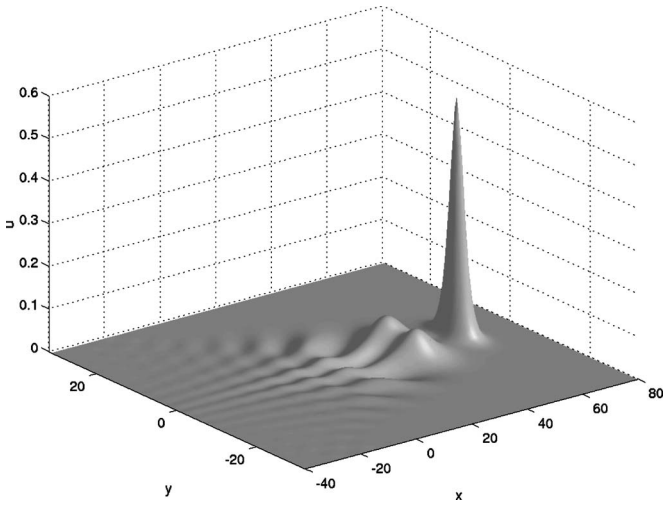

FIG. 2. Numerical solution of the electromigration equations (2) and (3) at $t=30$ for the initial condition (5) with $A=0.3$ and $\kappa=0.05$.

at the later time $t=25$. It is clear that the lump initial condition has evolved into a lump soliton followed by a tail of radiation within a caustic. This radiation propagates to the left, as expected since the group velocity for waves for the linearized ZK equation is negative. The lump eventually settles to a steady traveling wave after radiating away its excess mass and momentum. In addition it can be seen that at least one more soliton is developing from the radiation behind the initial lump. Very similar evolution for the coupled system of the ZK equation (2) and the potential equation (3) is observed in Fig. 2. The conclusion is that the surface displacement u drives the potential Ψ, which in turn modifies u. However, this modification is just in the velocity of u, due to the convective term. In the next section we shall turn to the derivation of the approximate equations for the ZK equation for the evolution of the initial condition (5).

III. APPROXIMATE EVOLUTION EQUATIONS

Let us first consider the modified ZK equation

$$\frac{\partial u}{\partial t}+6u^{p}\frac{\partial u}{\partial x}+\frac{\partial^{3}u}{\partial x^{3}}+\frac{\partial^{3}u}{\partial x\partial y^{2}}=0, \tag{8}$$

where again p must be a positive integer, together with the initial condition

$$u(x,y,0)=Ae^{-\kappa(x^{2}+y^{2})}. \tag{9}$$

In order to derive the approximate evolution equations for this initial condition, we proceed as in Refs. 10 and 11 by setting

$$u(x,y,t)=u_{0}+u_{1}=a(t)e^{-\kappa(t)[(x-\zeta(t))^{2}+y^{2}]}+u_{1}. \tag{10}$$

The position of the soliton is then $(\zeta(t),0)$, its amplitude is $a(t)$, and its width is $\kappa^{-1}(t)$. The function u_1 represents the radiation shed by the pulse as it evolves. The approximate equations governing the evolution of the pulse are now obtained by an appropriate use of the conservation equations (6) and (7), resulting in equations of motion for a, κ, and ζ. It is remarked that the procedure of Refs. 10 and 11 for the

KP and KdV equations, respectively, is a version of the modulation theory of Whitham[12] whereby the spatial modulations of the trial functions, which are not exact solutions, are neglected, but the relevant degrees of freedom of the shed radiation are included. Equations for the collective coordinates for both the lump and the shed radiation are then obtained.

As can be seen from Figs. 1(a) and 1(c) the lump part u_0 of u is separated from the radiation u_1 and the radiation is confined to a region bound by caustics. First the region of the radiation between the caustics then needs to be determined, as in Ref. 10. In order to determine this region, we again observe from Fig. 1 that $|u_1| \ll |u_0|$. The equation governing the radiation is therefore the linearized ZK equation

$$\frac{\partial u_1}{\partial t} + \frac{\partial^3 u_1}{\partial x^3} + \frac{\partial^3 u_1}{\partial x \partial y^2} = g(x - \zeta(t), y), \tag{11}$$

together with the initial condition $u_1(x,y,0)=0$. The term g on the right-hand side represents the source of radiation due to the pulse u_0. This source term is assumed to have small extent relative to the extent of the linear radiation u_1.

Assuming that ζ is slowly varying, the solution of the radiation equation (11) is

$$u_1(x,y,t) = \frac{1}{(2\pi)^2} \int_{-\infty}^{\infty} \int_{-\infty}^{\infty} U(k,l) e^{i\varphi(k,l,x,y,t)}\, dk dl, \tag{12}$$

where the phase φ is $\varphi = k(x-\zeta) + ly - \omega(k,l)t$ and the linear dispersion relation is $\omega = -k^3 - kl^2$. The kernel $U(k,l)$ is related to the source of radiation g. The actual form of U plays no role in the determination of the region of confinement of the radiation.

As for general linear dispersive wave theory,[12] the radiation is confined inside the caustics of (12). These caustics are determined by finding the evolution of u_1 for large time using the method of stationary phase. The points of stationary phase for the integral (12) are given by the solutions of

$$\begin{aligned} 0 &= \frac{\partial \varphi}{\partial k} = x - \zeta + (3k^2 + l^2)t, \\ 0 &= \frac{\partial \varphi}{\partial l} = y + 2klt. \end{aligned} \tag{13}$$

Solving for l using the second of these equations and substituting into the first gives the curves of constant wave number k as the family of parabolas

$$x - \zeta + \left(3k^2 + \frac{y^2}{4k^2 t^2}\right) t = 0. \tag{14}$$

The envelope of this family of parabolas is the curve of coalescence of stationary points, which is the caustic. To calculate the envelope, Eq. (14) and its derivative with respect to the parameter k are solved simultaneously for k. This gives the equation for the caustic as

$$x - \zeta(t) \pm \sqrt{3} y = 0. \tag{15}$$

The caustic is therefore straight lines forming a wedge with apex at the lump located at $(\zeta(t),0)$ and which trails behind it.

It should be noted that, unlike the situation for the KP equation,[10] the caustics do not change with time. The shed radiation is confined to the region between the caustics. This geometric argument then explains the radiation patterns in Fig. 1(c). Exactly the same calculation of the caustic is possible for the three space dimensional ZK equation. In this three-dimensional case, the caustic is a conical surface. The three-dimensional case will be taken up further in Sec. V. With this information about the location of the radiation, we can now determine the approximate equations for the parameters of the approximate lump solution (10).

Let us begin by determining an approximate lump solution of permanent form for the ZK equation. To this end we seek solutions of the form

$$u = v(x - ct, y). \tag{16}$$

Substituting this form into the modified ZK equation (8), it can be found, after an integration in x, that v satisfies the elliptic partial differential equation

$$-cv + \frac{6}{p+1} v^{p+1} + \frac{\partial^2 v}{\partial \eta^2} + \frac{\partial^2 v}{\partial y^2} = 0, \tag{17}$$

where $\eta = x - ct$. Now this elliptic equation is the Euler-Lagrange equation for the functional

$$F(v) = \int_{-\infty}^{\infty} \int_{-\infty}^{\infty} \left[\frac{1}{2}(v_\eta^2 + v_y^2) - \frac{6}{(p+1)(p+2)} v^{p+2} + \frac{c}{2} v^2 \right] d\eta dy. \tag{18}$$

At this stage the stability of the two-dimensional solitons could be analyzed following Refs. 13–15. To this end, one could use a trial function in the functional (18) which is the exact, but analytically unknown, soliton solution scaled to conserve momentum. The variation of the functional (18) evaluated along this scaled soliton will then give the stability region in parameter space, as in Refs. 13–15. However, in the present work, we are interested in not just the stability, but the dynamics of the approach to equilibrium, or departure from it. Hence we shall not proceed as in Refs. 13–15, but assume a trial function as in Ref. 11. However, a brief outline of the main ideas will now be given.

The functional in (18) is just the Hamiltonian with the momentum constrained with the velocity c as the Lagrange multiplier.[14,15] Therefore, to obtain a rigorous assessment of the stability of the two-dimensional soliton, we proceed as in Refs. 13–15. Let $u_s(x,y)$ be the exact extremum of the functional (18) constrained to the value P_0 of the momentum. Then consider the curve, in function space,

$$f_a(x,y) = \frac{1}{a} u_s(x/a, y/a). \tag{19}$$

This curve is the soliton solution when $a=1$ and satisfies the momentum constraint since

$$\int_{-\infty}^{\infty}\int_{-\infty}^{\infty} f_a^2\,dxdy = \int_{-\infty}^{\infty}\int_{-\infty}^{\infty} u_s^2\,dxdy = P_0. \tag{20}$$

Evaluation of the functional (18) along the curve f_a gives

$$F(f_a) = \frac{T}{a^2} - \frac{U}{a^p} + cP_0 = H(a) + cP_0, \tag{21}$$

where $H(a)$ is the Hamiltonian evaluated along the curve and

$$T = \frac{1}{2}\int_{-\infty}^{\infty}\int_{-\infty}^{\infty} |\nabla u_s|^2\,dxdy \quad \text{and}$$
$$U = \frac{6}{(p+1)(p+2)}\int_{-\infty}^{\infty}\int_{-\infty}^{\infty} u_s^{p+2}\,dxdy. \tag{22}$$

Clearly, by construction, $H(1)$ is an extremum of the Hamiltonian. The study of the nature of the Hamiltonian along the curve f_a amounts to a study of the stability of the critical point at $a=1$. To this end

$$H'(a) = -\frac{2T}{a^3} + \frac{pU}{a^{p+1}}, \tag{23}$$

which gives $H'(1)=0$ as $2T=pU$ at $a=1$. This also shows that the potential energy U is positive. The nature of the critical point is then determined by

$$H''(1) = T[6 - 2(p+1)]. \tag{24}$$

From the second derivative (24) it is clear that along the curve f_a the soliton solution is a minimum for $p<2$ and a maximum for $p>2$. The behavior at the critical value $p=2$ is not determined by this simple analysis and appears as a threshold in a similar way to other soliton equations treated in Refs. 14 and 15.

This analysis following Refs. 14 and 15 provides a rigorous result for the instability of the two-dimensional soliton. In the stable case it is not conclusive as all directions must be included to determine stability. However, the analysis provides a rigorous result in a restricted class of deformations in the stable case. Since in the present work we are interested in the study of the dynamics of the evolution of lump-type initial conditions, we shall now focus on determining approximate equations for the collective coordinates for both an approximate lump solution and the shed radiation which plays the essential role in stabilizing the lump solution of this infinite dimensional Hamiltonian system.

Let us now assume that the trial function v for the traveling wave solution (16) is the Gaussian

$$v = ae^{-\kappa(\eta^2+y^2)}. \tag{25}$$

Substituting this trial function into the Lagrangian (18), the average Lagrangian can be found to be

$$F(a,\kappa,c) = \frac{\pi}{2}a^2 - \frac{6\pi}{(p+1)(p+2)^2}\frac{a^{p+2}}{\kappa} + \frac{\pi c}{4}\frac{a^2}{\kappa}. \tag{26}$$

The variational equations F_a and F_κ for this averaged Lagrangian then have a stationary point given by

$$c = \frac{12}{(p+1)(p+2)}a^p - 2\kappa \quad \text{and} \quad a^p = \frac{(p+1)(p+2)^2}{6p}\kappa. \tag{27}$$

These equations give the velocity and amplitude of the fixed point, which is an approximate steady solitary wave solution of the modified ZK equation. It can be found that the velocity-amplitude relation for the solitary wave is

$$c = \frac{24}{(p+1)(p+2)^2}a^p. \tag{28}$$

This relation shows that there is a one-parameter family of approximate steady solitary wave solutions.

Using these results, the approximate equations for the solitary wave can now be determined. The first approximate equation is just the solitary wave velocity

$$\dot{\zeta} = V = c(a), \tag{29}$$

where c is given by (28). The remaining approximate equations for a and κ are found by using the conservation equations (6) and (7). The momentum conservation equation (7) gives

$$0 = \frac{d}{dt}\int_{-\infty}^{\infty}\int_{-\infty}^{\infty} u^2\,dxdy = \frac{d}{dt}\int_{-\infty}^{\infty}\int_{-\infty}^{\infty}(u_0^2 + 2u_0u_1 + u_1^2)\,dxdy. \tag{30}$$

Now, as can be seen from the numerical solutions of Fig. 1 and has been determined from the caustic derivation above, the radiation u_1 does not overlap the soliton u_0. Furthermore, as the radiation has small amplitude relative to the pulse, u_1^2 is negligible. Then, using the trial function (10) and the velocity expression (29), we have

$$\frac{d}{dt}\int_{-\infty}^{\infty}\int_{-\infty}^{\infty} u_0^2\,dxdy = \frac{d}{dt}\int_{-\infty}^{\infty}\int_{-\infty}^{\infty} a^2e^{-2\kappa[(x-\zeta)^2+y^2]}\,dxdy = \frac{d}{dt}\frac{\pi a^2}{2\kappa} = 0. \tag{31}$$

The equation for conservation of mass will then close the system of approximate equations (29) and (31).

Let us consider mass balance in the shaded region $R(t)$ shown in Fig. 3, which is the region outside the caustic. That is we calculate

$$\frac{d}{dt}\int_{R(t)} u\,dxdy. \tag{32}$$

Differentiating we obtain

$$\frac{d}{dt}\int_{R(t)} u\,dxdy = -2V\int_0^{\infty} u\Big|_{x=\eta-\sqrt{3}y} dy - \int_{R(t)}\frac{\partial}{\partial x}\left[\frac{6}{p+1}u^{p+1} + u_{xx} + u_{yy}\right]dxdy. \tag{33}$$

Since the region $R(t)$ does not include, by construction, the radiation, u can be replaced in this equation by the Gaussian

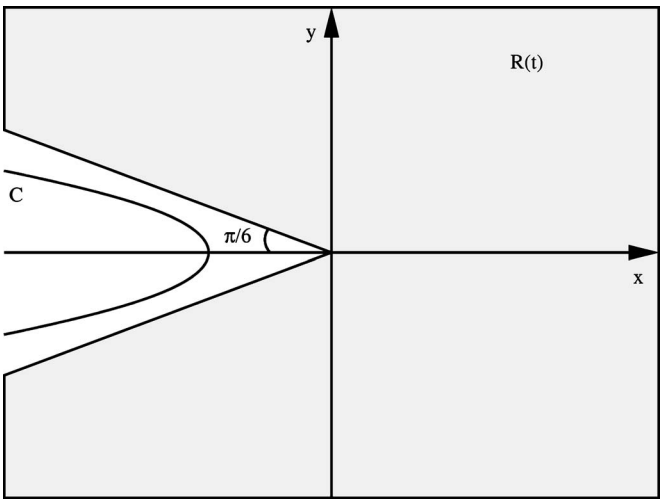

FIG. 3. Region $R(t)$ outside caustic.

lump in (10). The following expressions are then obtained for the various integrals in (33):

$$\int_{R(t)} u\,dxdy = \frac{5\pi}{6}\frac{a}{\kappa},$$

$$\int_0^\infty u\Big|_{x=\eta-\sqrt{3}y} dy = \frac{\sqrt{\pi}}{4}\frac{a}{\sqrt{\kappa}}, \tag{34}$$

$$\int_{R(t)} \frac{\partial}{\partial x}\left[\frac{6}{p+1}u^{p+1} + u_{xx} + u_{yy}\right] dxdy$$
$$= -2\int_0^\infty \left[\frac{6}{p+1}u^{p+1} + u_{xx} + u_{yy}\right]\Big|_{x=\eta-\sqrt{3}y} dy$$
$$= -2\sqrt{\pi}\left(\frac{6a^{p+1}}{4(p+1)^{3/2}\kappa^{1/2}} - \frac{a\kappa^{1/2}}{2}\right).$$

Using these expressions, the conservation equation (33) becomes

$$\frac{5\sqrt{\pi}}{6}\frac{d}{dt}\frac{a}{\kappa} = \frac{6a^{p+1}}{2(p+1)^{3/2}\sqrt{\kappa}} - \frac{V}{2}\frac{a}{\sqrt{\kappa}} - a\sqrt{\kappa}. \tag{35}$$

The system of equations (29), (31), and (35) governing the evolution of the pulse is a closed system of equations for the pulse amplitude a, the pulse width κ^{-1}, and the velocity $\dot{\zeta}=V$, which together describe its evolution. It is to be noted that when the velocity V in (27) obtained by the variational method is substituted into the mass conservation equation (35), the fixed point of this equation is $a=0$. This nonphysical situation arises from the fact that the Gaussian trial function (10) is not an exact solution of the ZK equation and thus the conservation equations and variational approximation need not give the same solution, as would be the case if the trial function was based on an exact solution of the governing equations. This difference is shown in Figs. 5(a) and 5(b). The same situation is encountered in other problems for which an approximate trial function is used to obtain approximate evolution equations. To overcome this nonphysical result, the velocity is now calculated by considering the evolution of the moment of momentum. This calculation is performed using the same approximations as were made in the derivation of the conservation equations, such as the mass equation (35).

From the ZK equation (8) it can be shown that the moment of momentum equation is

$$\frac{d}{dt}\int_{-\infty}^{\infty}\int_{-\infty}^{\infty}\frac{1}{2}xu^2\,dxdy = -\int_{-\infty}^{\infty}\int_{-\infty}^{\infty}\left[x\frac{\partial}{\partial x}\left(\frac{6}{p+2}u^{p+2} + uu_{xx} - \frac{1}{2}u_x^2 - \frac{1}{2}u_y^2\right) + \frac{\partial}{\partial y}(uu_{xy})\right] dxdy. \tag{36}$$

Using the trial function (10) and recalling that $u_0u_1=0$, that u_0 and u_1 and their derivatives are zero at infinity, and that $|u_1| \ll u_0$, we obtain

$$\frac{d}{dt}\left(\zeta\frac{a^2}{\kappa}\right) = \frac{24}{(p+2)^2}\frac{a^{p+2}}{\kappa} - 4a^2. \tag{37}$$

Using the momentum equation (31), this gives to leading order

$$\dot{\zeta} = V = \frac{24a^p}{(p+2)^2} - 4\kappa, \tag{38}$$

which specializes in the case $p=1$ to

$$\dot{\zeta} = V = \tfrac{8}{3}a - 4\kappa. \tag{39}$$

Therefore the closed system of approximate equations for the amplitude a, width κ^{-1}, and velocity $\dot{\zeta}=V$ is now

$$\frac{d}{dt}\frac{a^2}{\kappa} = 0 \quad \text{or} \quad \frac{a^2}{\kappa} = \frac{a_0^2}{\kappa_0}, \tag{40}$$

$$\frac{5\sqrt{\pi}}{6}\frac{d}{dt}\frac{a}{\kappa} = \frac{6a^{p+1}}{2(p+1)^{3/2}\sqrt{\kappa}} - \frac{V}{2}\frac{a}{\sqrt{\kappa}} - a\sqrt{\kappa}, \tag{41}$$

$$\dot{\zeta} = V = \frac{24a^p}{(p+2)^2} - 4\kappa. \tag{42}$$

They combine to give the single equation for the amplitude

$$\frac{5\sqrt{\pi}}{6}\frac{da}{dt} = \frac{\kappa_0^{1/2}}{a_0}\left[\sigma(p)a^p - \frac{\kappa_0}{a_0^2}a^2\right]a^2, \tag{43}$$

where $a(0)=a_0$, $\kappa(0)=\kappa_0$, and

$$\sigma(p) = \frac{12}{(p+2)^2} - \frac{3}{(p+1)^{3/2}}. \tag{44}$$

For $p=1$ there is a stable fixed point given by

$$a_e = \sigma(1)\frac{a_0^2}{\kappa_0} = \frac{8\sqrt{2}-9}{6\sqrt{2}}\frac{a_0^2}{\kappa_0}. \tag{45}$$

It is important to note that the equilibrium amplitude a_e will be attained in different ways according to the relationship between the initial amplitude and width. If $0<\kappa_0<\sigma(1)a_0$,

the initial Gaussian u_0 will absorb mass until it reaches a lump with amplitude a_e; if $\kappa_0 > \sigma(1)a_0$, the initial Gaussian will lose mass until it stabilizes to a Gaussian of amplitude a_e. The special case $\kappa_0 = \sigma(1)a_0$ for the initial Gaussian will show very small changes with time.

For other values of p, it is convenient to write the amplitude equation (43) in the form

$$\frac{5\sqrt{\pi}}{6}\frac{da}{dt} = \frac{\kappa_0^{1/2}}{a_0}\left[\sigma(p) - \frac{\kappa_0}{a_0^2}a^{2-p}\right]a^{p+2}, \quad 0 < p < 2, \quad (46)$$

$$\frac{5\sqrt{\pi}}{6}\frac{da}{dt} = \frac{\kappa_0^{1/2}}{a_0}\left[\sigma(p)a^{p-2} - \frac{\kappa_0}{a_0^2}\right]a^4, \quad 2 \leqslant p. \quad (47)$$

The physical fixed point for the amplitude equation (46) is

$$a_e = \left(\frac{a_0^2}{\kappa_0\sigma(p)}\right)^{1/(2-p)} \quad (48)$$

and a similar time evolution behavior as the one described above for $p=1$ occurs. Nevertheless, for the amplitude equation (47) for $p \geqslant 2$ a more careful analysis must be made. Since $\sigma(p) < 0$ for $p > 10.44$, the amplitude equation (47) predicts a final lump solution with amplitude

$$a_e = \left[\frac{\kappa_0}{a_0^2\sigma(p)}\right]^{1/(p-2)} \quad (49)$$

for $2 < p < 10.44$, but when $p > 10.44$ the steady lump ceases to exist. Also for $0 < p < 2$ the fixed point is stable, while for $2 < p < 10.44$ it is unstable.

For the case $p=2$, the only fixed point is $a=0$ and the exact solution of the approximate equation (47) for the pulse amplitude is

$$a(t) = \frac{a_0}{[1 - (18/5\sqrt{\pi})a_0^2\kappa_0^{1/2}(\sigma(2) - \kappa_0/a_0^2)t]^{1/3}}. \quad (50)$$

If the initial conditions for the width and amplitude satisfy $\kappa_0 < \sigma(2)a_0^2$, then the initial Gaussian reaches infinite amplitude at time

$$t^* = \frac{5\sqrt{\pi}}{18a_0^2\kappa_0^{1/2}[\sigma(2) - \kappa_0/a_0^2]}. \quad (51)$$

On the other hand, if $\kappa_0 > \sigma(2)a_0^2$, then the initial Gaussian decays into radiation. This unstable behavior for $p \geqslant 2$ will also be studied numerically in Sec. VI. Similar behavior for the mKdV equation was observed in Ref. 8 and studied using the present approximate method in Ref. 9. In the threshold case $\kappa_0 = \sigma(2)a_0^2$, the approximate equations predict that this particular initial Gaussian (10) will change by a small amount. These results are of particular interest since in Ref. 8 the collision of two solitary waves traveling in the same direction for the case $p=2$ was studied. It was found that one of the waves blows up in finite time after interaction. In the present model we have finite time blow up for a family of initial Gaussians, independent of any interaction. The results of Ref. 8 can then be qualitatively explained by noting that the interaction increases the mass of the leading soliton above the threshold described above.

The solution of the amplitude approximate equation (43) for $p=1$ was compared with a full numerical solution of the ZK equation (1) for the same initial conditions as in Fig. 1. The agreement was found to be only qualitative, as expected from previous studies of the KdV equation[11] and the mKdV equation[9] where similar behavior was found. To overcome this a more accurate mass and momentum balance will now be analyzed in order to obtain approximate equations which include the effect of the shed dispersive radiation.

However, before considering a more detailed balance of mass and momentum, let us examine the expression (42) for the velocity. Previous work on the KdV,[11] mKdV,[9] KP,[10] and BO[16] equations shows that the velocity expression arising from the moment of momentum equation is the same as that of the variational formulation. However, it was further found that this velocity expression needed to be slightly modified in order to obtain the correct, numerical rate of decay to the fixed point. In this previous work it was argued that the correct velocity had the same functional form and fixed point as the one obtained by the approximate theory, but the coefficients had to be modified in order to give the correct timescale. For the cases of the BO and KP equations, the range of the coefficients was restricted so that the velocity was nonsingular. For the KdV and mKdV equations, the single free parameter in the velocity expression was obtained by matching to a specific numerical solution and excellent agreement with full numerical solutions was then obtained for a very wide range of initial values. This procedure was suggested by analogy with other mechanical problems. We note that the velocity is an angle variable. We recall from the theory of mechanical systems that an angle variable evolving in a system with a mean level, such as an oscillator with a quadratic nonlinearity, will have its evolution coupled to the mean level. The final form for the velocity will then have the functional form appropriate for the self-interaction, but with coefficients modified by the mean level. What is not clear is how to compute the localized mean level which couples to the velocity. However, we shall assume the same result valid for simple systems and verify its validity by comparison with full numerical solutions. It is in our view a very interesting problem of how to develop the appropriate perturbation theory to account for this effect. It is noted that in the present case the velocity expression (42), which gives the nontrivial fixed point, is the one modified.

In order to preserve the fixed point of the approximate equation (41), expression (42) for the velocity V is modified as

$$V = \mu a^p - 4\kappa + \left[\frac{24}{(p+2)^2} - \mu\right]\frac{\kappa}{\sigma(p)}, \quad (52)$$

where $\sigma(p)$ was defined above as

$$\sigma(p) = \frac{12}{(p+2)^2} - \frac{3}{(p+1)^{3/2}}. \quad (53)$$

This specializes in the case $p=1$ to

$$V = \mu a - 4\kappa + \left(\frac{8}{3} - \mu\right)\frac{\kappa}{\sigma(1)}. \tag{54}$$

A vital point is that the fixed point of the approximate equations does not depend on the value of μ. These velocity expressions reduce to the fixed point value (39) when a and κ satisfy the fixed point relation $\kappa = \sigma(p)a^p$, independent of the value of μ.

To obtain a more detailed momentum balance we see that the radiation shed by the evolving lump transports momentum away from it. The momentum conservation equation (31) does not account for this loss. To include this loss of momentum by the lump, let us consider momentum balance in the region $\Gamma(t)$ which lies to the right of the curve C of Fig. 3 [including the region $R(t)$]. Then from the modified ZK equation (8) it can be found that

$$\frac{d}{dt}\int_{\Gamma(t)} \frac{1}{2}u^2\, dxdy = \int_{C(t)} \left(\frac{u^{p+2}}{p+2} + uu_{xx} - \frac{1}{2}u_x^2 - \frac{1}{2}u_y^2, uu_{xy}\right)\cdot \mathbf{n}\, dS - V\int_{C(t)} \frac{1}{2}u^2\, dS. \tag{55}$$

Here $\mathbf{n}$ is the outward unit normal to $C(t)$. To derive this momentum balance equation it has been assumed that the curve $C(t)$ moves rigidly with the velocity V of the lump.

It can be seen from Fig. 1 that as the lump evolves, a flat shelf, of small amplitude relative to the lump, forms, which is attached behind the lump. Let the amplitude of this flat shelf be u_∞. Since the shelf is flat and the derivative terms in the momentum balance equation (55) are quadratic, they can be neglected. Evaluating the integral on the left-hand side of (55) using the trial function of (10), we then have

$$\frac{d}{dt}\frac{\pi}{4}\frac{a^2}{\kappa} = -\int_{C(t)} \left(\frac{u_\infty^{p+2}}{p+2} + \frac{1}{2}Vu_\infty^2\right) dS. \tag{56}$$

This momentum equation gives the momentum lost from the lump to the shed dispersive radiation. Finally, if it is assumed that the length of the curve C for which the shelf is flat is ℓ and that p is larger than 1, the momentum balance equation for the lump is

$$\frac{d}{dt}\frac{\pi a^2}{\kappa} = -2V\ell u_\infty^2. \tag{57}$$

To conclude the momentum balance equation, we need to determine the amplitude u_∞ of the shelf by relating it to the mass lost by the lump. To this end, we reconsider mass balance, including the trailing flat shelf. Now the shelf is bounded by a caustic. Therefore, as for momentum balance, it can be shown from the modified ZK equation (8) that the mass balance equation is

$$\frac{d}{dt}\int_{\Gamma(t)} u\, dxdy = -\int_{C(t)} \left(\frac{u^{p+1}}{p+1} + u_{xx} + u_{yy}\right) dS - V\int_{C(t)} u\, dy. \tag{58}$$

To derive this mass balance expression it has again been assumed that the shelf is rigidly attached to the lump and moves with velocity V.

As above, we now take the shelf to be flat and to have small amplitude relative to the lump, as is illustrated in Fig. 1(b), and take u_∞ to be the amplitude of the shelf at C. Therefore, as for momentum conservation, the derivatives in (58) can be neglected. Then calculating the mass of the lump from the trial function in (10), we have

$$\frac{d}{dt}\frac{\pi a}{\kappa} = -\int_C \left(\frac{u_\infty^{p+1}}{p+1} + Vu_\infty\right) dS. \tag{59}$$

The integral on the right-hand side of this mass balance equation is again approximated by taking the length of the curve C for which the shelf is flat to be ℓ, so that the final mass balance equation for the evolution of the lump is

$$\frac{d}{dt}\frac{\pi a}{\kappa} + \ell u_\infty\left(V + \frac{u_\infty^p}{p+1}\right) = 0. \tag{60}$$

This equation determines the mass of the lump, incorporating the mass lost from the lump to the shed dispersive radiation. Since we are interested in the case for which $p \geqslant 1$ and $u_\infty \ll 1$, we have

$$u_\infty = -\frac{1}{\ell V}\frac{d}{dt}\frac{\pi a}{\kappa}, \tag{61}$$

which is the same expression for the shelf amplitude as for the KP equation.[10] Using this expression for u_∞ in the momentum balance equation (57) gives the final momentum equation for the lump as

$$\frac{d}{dt}\frac{\pi a^2}{\kappa} + \frac{2}{\ell V}\left(\frac{d}{dt}\frac{\pi a}{\kappa}\right)^2 = 0. \tag{62}$$

This momentum equation, together with the mass equation (35), is the system of approximate equations for the evolution of the lump.

The system of approximate equations (35) for mass, (52) for the velocity, and (62) for momentum form a closed system of equations for the lump amplitude a and width κ^{-1}, which are the collective coordinates. It is noted that the family of fixed points is independent of ℓ and μ. Solutions of this system of approximate equations will be compared with full numerical solutions of the modified ZK equation in Sec. VI. Before these numerical and approximate results are compared, the approximate equations for the three-dimensional case will be derived in the next section.

IV. EXTENSION TO THREE SPACE DIMENSIONS

Due to the simplicity of the caustic and the trial function for the ZK equation, it is possible to extend the calculation of the approximate equations to the three space dimensional version of the ZK equation. To this end, the three-dimensional trial function

$$u_0 = a(t)e^{-\kappa[(x-\zeta(t))^2+y^2+z^2]} \tag{63}$$

is used for the three-dimensional ZK equation (4). Exactly the same procedure as for the two-dimensional ZK equation can be carried out, based on equations for conservation of

mass and momentum. The caustic is now a surface, but since this caustic surface is conical and the trial function is Gaussian, the integrals involved in averaging the conservation equations can be carried out in detail.

With these extensions to three space dimensions, the approximate equations for the evolution of a lump for the three-dimensional ZK equation (4) are, as before, obtained from the equations for conservation of mass and momentum and the equation for moment of momentum in the form

$$\sqrt{\pi}\left(1+\frac{\sqrt{3}}{2}\right)\frac{d}{dt}\frac{a}{\kappa^{3/2}}=\frac{1}{2(1+p)^2}\frac{a^{1+p}}{\kappa}-\frac{Va}{2\kappa}-a, \tag{64}$$

$$\frac{d}{dt}\frac{a^2}{\kappa^{3/2}}=0, \tag{65}$$

$$V=\frac{4\sqrt{2}}{(2+p)^{5/2}}a^p-5\kappa, \tag{66}$$

when the loss of momentum to the shed radiation is neglected. As before, V denotes the velocity. It is possible to reduce these approximate equations to a single equation for the pulse amplitude a in terms of the initial values a_0 for a and κ_0 for κ. This equation is

$$\frac{da}{dt}=\frac{\sqrt{\kappa_0}}{a_0^{3/2}}\left(\gamma(p)-\beta\frac{\kappa_0}{a_0^{4/3}}a^{4/3-p}\right)a^{p+5/3},\quad 0\leqslant p<\frac{4}{3}, \tag{67}$$

$$\frac{da}{dt}=\frac{\sqrt{\kappa_0}}{a_0^{3/2}}\left(\gamma(p)a^{p-4/3}-\beta\frac{\kappa_0}{a_0^{4/3}}\right)a^3,\quad \frac{4}{3}\leqslant p, \tag{68}$$

where the function γ is

$$\gamma(p)=\pi^{-1/2}\left(1+\frac{\sqrt{3}}{2}\right)^{-1}\left[\frac{2\sqrt{2}}{(2+p)^{5/2}}-\frac{1}{2(1+p)^2}\right], \tag{69}$$

and

$$\beta=\frac{3}{2\sqrt{\pi}}\left(1+\frac{\sqrt{3}}{2}\right)^{-1}. \tag{70}$$

A straightforward analysis of these equations shows that for $p<\frac{4}{3}$ the lump soliton fixed point is stable and is approached asymptotically. On the other hand, for $\frac{4}{3}\leqslant p\leqslant 25.61$ the soliton fixed point

$$a_e=\left(\frac{\beta}{\gamma(p)}\frac{\kappa_0}{a_0^{4/3}}\right)^{1/(p-4/3)} \tag{71}$$

acts as a threshold. Lumps with initial amplitudes below this threshold decay into radiation and lumps with initial amplitudes above the threshold narrow and collapse in finite time. Finally, for $p>25.61$, the soliton fixed point ceases to exist and all initial conditions decay into radiation. This behavior has not been verified numerically due to the amount of calculation required in three space dimensions and is beyond the scope of the present work. Finally in this section, the argument used to include the effects of shed dispersive radiation in the momentum equation will now be outlined.

Let us consider the mass conservation equation for the total of the mass of the lump and the mass M_1 of the radiation

$$\pi^{3/2}\frac{d}{dt}\frac{a}{\kappa^{3/2}}+\frac{dM_1}{dt}=0. \tag{72}$$

As in the two-dimensional case of the previous section, it is assumed that a shelf of cross-sectional area A and of approximately constant amplitude $u=u_\infty$ is formed inside the caustic surface which travels at the same velocity V of the lump. Assuming $|u_\infty|\ll 1$, then the approximate equations for the three-dimensional pulse can be derived in the same manner as for the two-dimensional equations (33)–(35). In particular, as for the two-dimensional mass equation (59), the derivative of the radiation mass M_1 can be approximated by

$$\frac{dM_1}{dt}=\frac{6A}{p+1}u_\infty^{p+1}+VAu_\infty. \tag{73}$$

We thus obtain

$$\pi^{3/2}\frac{d}{dt}\frac{a}{\kappa^{3/2}}+\frac{6A}{p+1}u_\infty^{p+1}+VAu_\infty=0. \tag{74}$$

The conservation of momentum equation, including momentum loss to radiation, is obtained in a similar manner as for the two-dimensional case of the previous section, with A and u_∞ as for mass conservation,

$$\frac{\pi^{3/2}}{4\sqrt{2}}\frac{d}{dt}\frac{a^2}{\kappa^{3/2}}+\frac{6A}{p+2}u_\infty^{p+2}+\frac{1}{2}AVu_\infty^2=0. \tag{75}$$

The same velocity expression (66) obtained on neglect of momentum loss to radiation is now used for the velocity V, since momentum loss to radiation is small.[11] The resulting equations for the evolution of the three-dimensional pulse are then

$$\pi^{3/2}\frac{d}{dt}\frac{a}{\kappa^{3/2}}+\frac{6A}{p+1}u_\infty^{p+1}+VAu_\infty=0, \tag{76}$$

$$\frac{\pi^{3/2}}{4\sqrt{2}}\frac{d}{dt}\frac{a^2}{\kappa^{3/2}}+\frac{6A}{p+2}u_\infty^{p+2}+\frac{1}{2}AVu_\infty^2=0, \tag{77}$$

$$V=\frac{4\sqrt{2}}{(p+2)^{5/2}}a^p-5\kappa. \tag{78}$$

V. APPROXIMATE EQUATIONS FOR SURFACE ELECTROMIGRATION

The derivation of the approximate equations for surface electromigration, governed by the ZK equation (2) and Poisson's equation (3), is very similar to that for the modified ZK equation of the previous section. Therefore, only the main changes from the derivation of the previous section will be discussed in detail. As was remarked at the end of Sec. II, comparing Figs. 1 and 2 shows that lump evolution for the ZK equation (1) is very similar to that for the coupled system (2) and (3) for electromigration. The only change is due to the convective term $\nabla u\cdot\nabla\Psi$. The system (2) and (3) again

conserves mass and momentum, so that these conservation equations will be used to derive the approximate equations.

The trial function to be used for u is the same as that for the ZK equation

$$u_0 = a(t)e^{-\kappa(t)[(x-\zeta(t))^2+y^2]}, \tag{79}$$

and the trial function for Ψ is the decaying solution of

$$\nabla^2\Psi_0 = \frac{\partial u_0}{\partial x}. \tag{80}$$

The solution of this Poisson equation for Ψ_0 is readily obtained by separation of variables as

$$\Psi_0 = \frac{a(t)(1-e^{-\kappa r^2})\cos\theta}{2r\kappa(t)} \tag{81}$$

in polar coordinates centred at $(\zeta(t),0)$. We now proceed as for the modified ZK equation of the previous section and use the trial functions (79) and (81) plus the equations for mass and momentum conservation to derive approximate equations for the evolution of the lump solution for electromigration.

Multiplying the ZK equation (2) by u and averaging by integrating the result over the region $R(t)$ of Fig. 3, we obtain the same momentum conservation equation as for the single ZK equation

$$\frac{d}{dt}\frac{\pi}{4}\frac{a^2}{\kappa} = 0. \tag{82}$$

Integrating the ZK equation (2) over the region $R(t)$, the mass conservation equation, modified by the convective term $\nabla u\cdot\nabla\Psi$,

$$\begin{aligned}\frac{d}{dt}\int_{R(t)} u\,dxdy = &-2V\int_0^\infty u\Big|_{x=\zeta-\sqrt{3}y}dy\\ &-2\int_0^\infty [3u^2+u_{xx}+u_{yy}]_{x=\zeta-\sqrt{3}y}\,dy\\ &+\frac{1}{2}\int_{R(t)}\nabla u\cdot\nabla\Psi\,dxdy\end{aligned} \tag{83}$$

is obtained. To evaluate the integrals in (83) the trial functions (79) and (81) are used to obtain a mass equation similar to (35) for the single ZK equation, but modified by the convective term. The result is

$$\frac{5\sqrt{\pi}}{6}\frac{d}{dt}\frac{a}{\kappa} = \frac{15-2\sqrt{2}}{8\sqrt{2}}\frac{a^2}{\sqrt{\kappa}} - \frac{Va}{2\sqrt{\kappa}} - a\sqrt{\kappa}. \tag{84}$$

To complete the approximate equations, an expression for the velocity V is needed. Calculating this expression from the moment of momentum equation for the electromigration ZK equation (2) gives the same expression (39) in a and κ as for the ZK equation (1), but with modified coefficients

$$V = \tfrac{49}{18}a - 4\kappa. \tag{85}$$

With this velocity expression the mass conservation equation (84) has the fixed point

$$\kappa = \rho a \quad \text{with} \quad \rho = \frac{482\sqrt{2}-540}{288\sqrt{2}}. \tag{86}$$

Again, as in Refs. 9–11, to obtain good agreement with full numerical solutions for the rate of decay of the solution of the approximate equations onto the fixed point, this velocity expression is modified with a free parameter μ. Modifying the velocity expression as for the modified ZK equation results in

$$V = \mu a - 4\kappa + \left(\frac{49}{18}-\mu\right)\frac{\kappa}{\rho}. \tag{87}$$

To include the momentum shed in the dispersive radiation behind the lump in the momentum equation (82), we proceed as in the previous section for the single ZK equation. It will be found in Sec. VI that the momentum shed in dispersive radiation is now larger than for the ZK equation. This is due to the algebraic decay of the solutions of Poisson's equation (3), which in turn produces a larger amount of dispersive radiation. Hence the momentum conservation equation (62) will be used to close the system of approximate equations (84) and (87).

VI. RESULTS

In the present section solutions of the approximate equations (35), (52), and (62) for the modified ZK equation (8) and the approximate equations (62), (84), and (87) for electromigration will be compared with full numerical solutions of the relevant governing equations. The modified ZK equation (8) and the ZK equation (2) for electromigration were solved numerically using a pseudo-spectral method based on that of Ref. 17, while the Poisson equation (3) for electromigration was solved using the spectral method of Ref. 18 based on fast Fourier transforms (FFTs). The approximate equations were solved numerically using the standard fourth-order Runge-Kutta scheme.

Figure 4 shows comparisons of the lump amplitude as given by solutions of the approximate equations (35), (52), and (62) for the ZK equation (for $p=1$) and by full numerical solutions of the ZK equation (1). The parameters μ and ℓ were chosen by matching the approximate solution to the numerical solution for the case shown in Fig. 4(a), for which the initial amplitude and width are $A=0.4$ and $\kappa=0.05$. The velocity parameter μ is a time constant for the approximate solution and just changes the rate of approach to the steady state and not the actual steady state value. The momentum loss parameter ℓ slightly modifies the steady state of the approximate equations as it is a small loss term. However, ℓ was taken to be 300, which shows that momentum loss to radiation is negligible for the ZK equation, and ℓ could be taken to be ∞, so that momentum is conserved by the pulse. The final, steady pulse amplitude increases quadratically with the initial amplitude, as can be seen from the momentum equation (62) with $\ell=\infty$. An amplitude comparison for the higher initial amplitude $A=0.5$ is shown in Fig. 4(b) and it can be seen that the final numerical amplitude has increased from 0.5 to approximately 1.2, so that the lump has increased in amplitude by approximately 2.5, while in Fig.

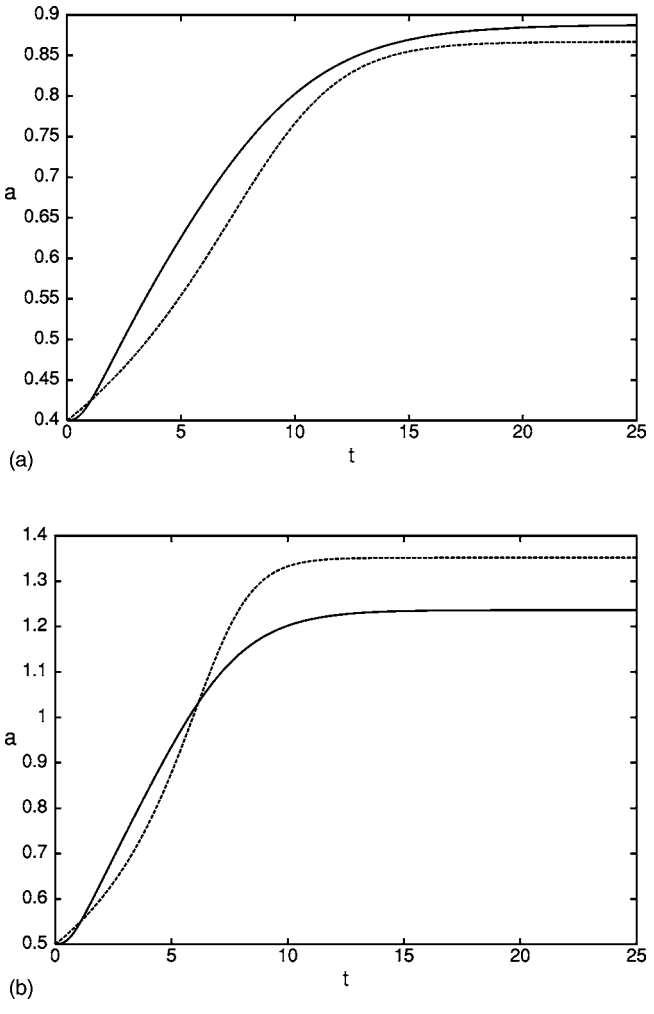

FIG. 4. Amplitude comparison between the numerical solution of the ZK equation (1) and the approximate equations (35), (62), and (52). The free parameters are $\mu=5.6$ and $\ell=300$. Numerical solution:———. Approximate solution:– – –. (a) Initial conditions $A=0.4$, $\kappa=0.05$. (b) Amplitude a for initial conditions $A=0.5$, $\kappa=0.05$.

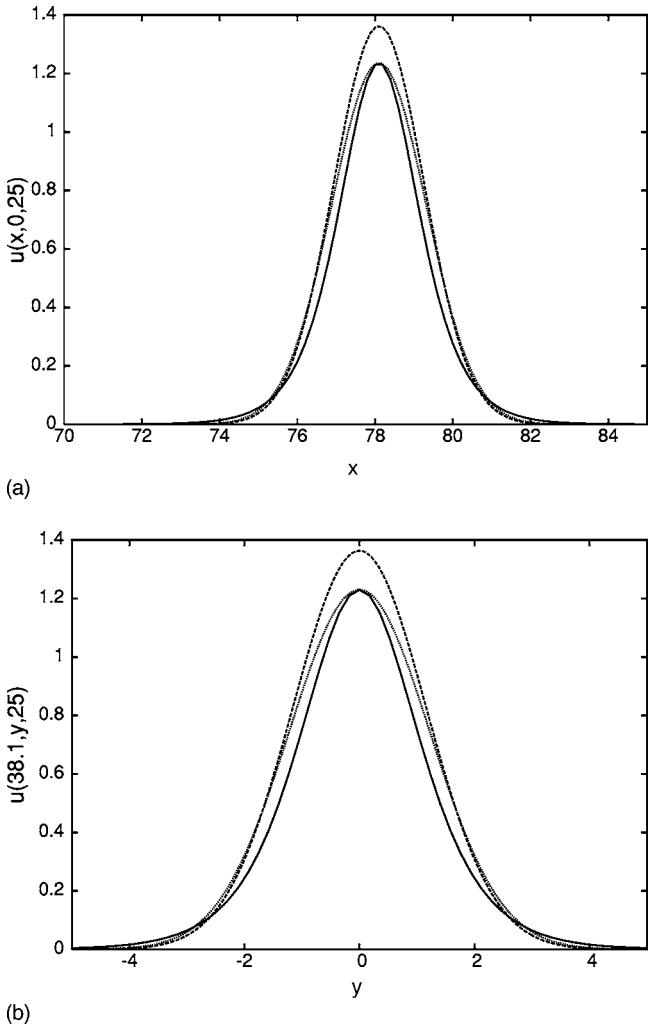

FIG. 5. Cross sections through the numerical solution of the ZK equation (1) at $t=25$ for the initial conditions $a=0.5$ and $\kappa=0.05$. Numerical solution:———. Gaussian u_0 in (10) with amplitude $a=1.36335$ from approximate solution:– – –. Gaussian u_0 in (10) with amplitude $a=1.2366$ from numerical solution:---. (a) Cross section through $y=0$. (b) Cross section through $x=40.0$ (at lump maximum).

4(a) the lump increased in amplitude by approximately 2. The approximate solution was calculated with the same values of μ and ℓ as for Fig. 4(a). It can be seen that even with this larger increase in amplitude, the agreement between the approximate and numerical solutions is still good, considering the approximations made in obtaining the approximate equations. Similar agreement between the numerical and approximate solutions is also obtained for initial amplitudes below $A=0.4$, so detailed comparisons for such lower amplitudes will not be shown here. It is noted that changing the value of the momentum loss parameter ℓ will not improve the agreement as decreasing ℓ from the large value taken will only decrease the amplitude due to increased loss.

The trial function for u_0 in (10) was taken to be Gaussian, mainly because the integrals involved in calculating the approximate equations could then be evaluated and because there is no exact soliton solution of the ZK equation on which to base a trial function. Figure 5(a) shows a section $y=0$ through the numerical solution at $t=25$ for the initial conditions $A=0.5$ and $\kappa=0.05$. Also shown are Gaussians u_0 from (10) with both an amplitude from the approximate solution at $t=25$ and from the numerical solution at $t=25$. The widths κ in these Gaussians are determined from the fixed point relation $\kappa=\sigma(p)a$. It can be seen that to a good approximation the lump is Gaussian, even for an initial condition for which the amplitude agreement is not so good. The corresponding cross section in the y direction through the lump maximum is shown in Fig. 5(b), with the agreement with the assumed Gaussian profile being similar to that for the x cross section. It can be seen that the difference in the profiles of the approximate and numerical solutions (for example, in the pulse width) is of the same order as the difference between the amplitude of the pulse as given by the these two solutions, as shown in Fig. 4(b). The use of the approximate pulse profile (10) is then a major cause of the differences between the approximate and numerical solutions.

The approximate equations for the modified ZK equation (35), (52), and (62) predict that the ZK soliton is unstable for $p\geqslant 2$. This is illustrated in Fig. 6(a) where the amplitude of the lump as given by the full numerical solution and the

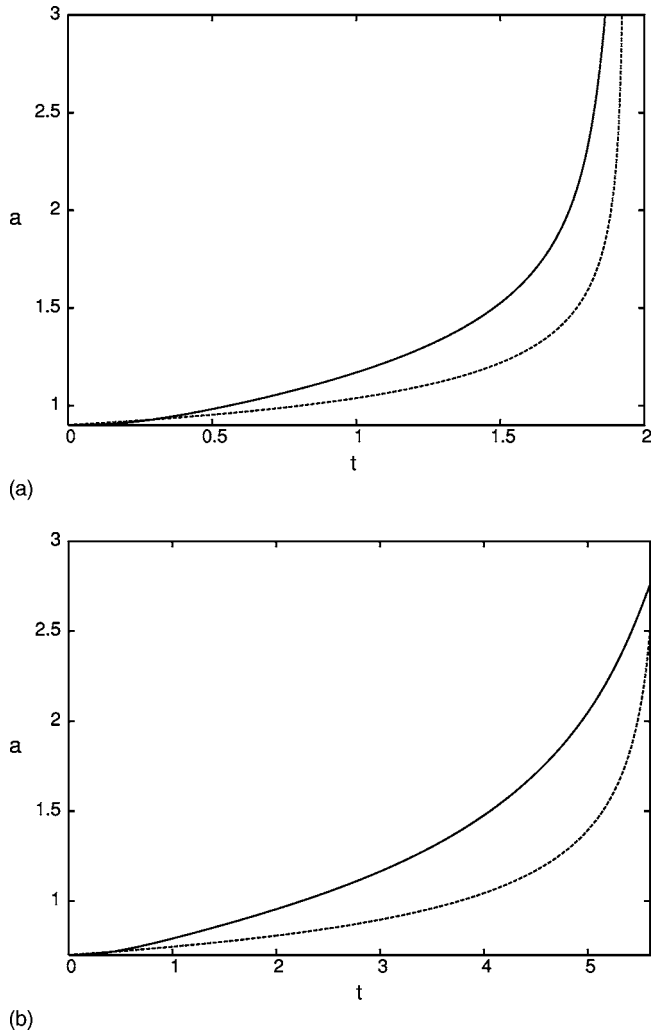

FIG. 6. Comparison between amplitude a of the lump as given by the numerical solution of the modified ZK equation (8) and the approximate equations (35), (62), and (52). Numerical solution:———. Approximate solution:– – –. (a) $p=3$, $\mu=6$ for initial values $A=0.9$ and $\kappa=0.05$. (b) $p=2$, $\mu=5.07$ for initial values $A=0.7$ and $\kappa=0.05$.

solution of the approximate equations for $p=3$ and for the initial values $A=0.9$ and $\kappa=0.05$ is shown. This initial value is above a ZK soliton as given by the approximate equations, so these approximate equations predict that the lump's amplitude will blow up as its width decreases to zero. It can be seen that the amplitude as given by the full numerical solution is blowing up, as predicted. Furthermore, there is excellent, even remarkable, agreement between the amplitude as given by the approximate equations and the numerical solution, with the blow-up time well predicted by the approximate equations. An amplitude comparison for the borderline case $p=2$ between stability and instability is shown in Fig. 6(b). The soliton for this borderline case is seen to be unstable. Again the comparison between the numerical and approximate solutions is excellent, even for a case for which the amplitude of the pulse rapidly blows up.

The final comparisons to be made are between full numerical solutions of the electromigration equations (2) and (3) and the approximate equations (62), (64), and (87) for these equations. Figure 7 shows an amplitude comparison

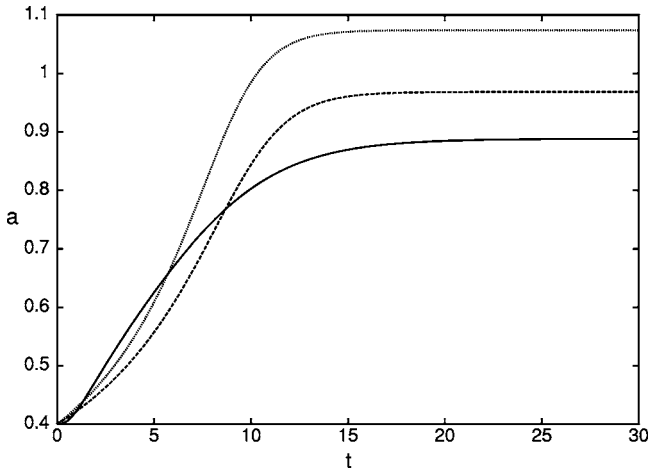

FIG. 7. Comparison between amplitude a of the lump as given by the numerical solution of the electromigration equations (2) and (3) and the approximate equations (82), (84), and (87). The free parameters are $\mu=5.6$ and $\ell=25$. Initial conditions are $A=0.4$, $\kappa=0.05$. Numerical solution:———. Approximate solution with momentum loss to radiation:– – –. Approximate without momentum loss to radiation: ---.

between the full numerical and approximate solutions for the initial amplitude $A=0.4$ and the initial width $\kappa=0.05$. In the present case of the electromigration equations the loss of momentum to dispersive radiation is significant, as can be seen by comparing Figs. 1(c) and 2, which shows that the radiation behind the lump for the electromigration equations has larger amplitude than for the ZK equation. The time constant μ and the momentum loss coefficient ℓ were chosen by matching with the full numerical solution for the initial amplitude $A=0.3$ and initial width $\kappa=0.05$, giving $\mu=5.6$, as for the ZK equation, and $\ell=25$. Since the comparison in this reference case is similar to that for the reference case for the ZK equation shown in Fig. 4(a), it is not shown here. The lower value of ℓ shows that momentum loss to the shed radiation must be included in order to obtain good agreement with the full numerical solution. In Fig. 7 the initial amplitude is increased to $A=0.4$ and it is again seen that momentum loss to radiation must be included to obtain agreement with the numerical solution. The disagreement between the approximate and numerical solutions in this higher amplitude case is similar to that shown in Fig. 4(b) for the ZK equation.

It is noted that the approximate equations were derived using mass conservation in the region $R(t)$ of Fig. 3. A major assumption was that the caustic opens immediately. However, this is not the case, as can be seen from examining Fig. 1(a), which shows a full numerical solution of the ZK equation (1) at $t=10$. This assumption of the immediate formation of the caustic is another reason for the discrepancy in the amplitude comparisons of Figs. 4, 6, and 7. Figures 1 and 2 show numerical solutions for cases where the fixed point amplitude is above the initial amplitude, in which case positive mass is shed behind the lump. For the KdV equation, such positive mass would evolve into a soliton.[12] It can be seen that a similar process is occurring in Figs. 1(c) and 2, where two smaller lumps are forming behind the main lump. It is not clear how to develop an asymptotic theory to describe the formation and evolution of these generated lumps.

VII. CONCLUSIONS

The asymptotic evolution of lump initial conditions into solitons has been studied for the two space dimensional ZK equation and for the system of a ZK equation and a Poisson equation governing electromigration. This work is complementary to that of Ref. 11 for the KdV equation, Ref. 9 for the mKdV equation, and Refs. 8 and 10 for the KP equation, where stability and threshold phenomena, if any, were studied asymptotically and numerically. It is again found that a geometric optics approach to the calculation of the effect of shed dispersive radiation on the evolution of the lump gives radiation damping in the approximate equations which results in good agreement between their solutions and full numerical solutions. As in previous work,[9–11,16] this is the consistency test for the choice of the conservation laws used to derive the approximate equations. In principle, one could use the equation for moment of mass and the energy conservation equation to derive the approximate equations. However, as in previous work,[9–11,16] the effect of the shed dispersive radiation is amplified on using the moment of mass equation, while the effect of the shed dispersive radiation is of lower order for the moment of momentum equation. Furthermore, the equation for conservation of energy is not sensitive enough to capture the deceleration of the pulse due to radiation loss. Finally, it was decided not to use the local conservation law for

$$\int_{-\infty}^{\infty} u(x,y,t)\,dx, \tag{88}$$

since it is assumed that the trial function satisfies the governing equation on average. The use of such a local conservation law, coupled with a different trial function, should be the subject of further work. While the damping terms contained free parameters, it was found that, as in previous studies,[9–11] once these parameters were fixed for one initial condition, good agreement was found for other initial conditions using these parameter values.

The approximate equations for the three space dimensional ZK equation predict broadly similar behavior to that for two dimensions. However, these three-dimensional approximate equations predict that for large nonlinearity p an initial condition will always decay into radiation.

The analysis of the present work predicts that for quadratic nonlinearity uu_x, i.e., $p=1$, which is the case relevant to the electromigration of small lumps on the surface of materials, small lumps will always evolve into solitons. This behavior is similar to that for the (one space dimensional) KdV equation.[12]

We end by remarking that the present work shows that complicated lump evolution can be captured accurately by systems of ordinary differential equations with few degrees of freedom.

ACKNOWLEDGMENTS

The authors gratefully acknowledge Grant No. CONACYT G25427-E for providing support for the visit of Dr. N. F. Smyth. The authors also acknowledge Ana Cecilia Perez for computing support and Professor A. A. Minzoni for several enlightening conservations about the present work. Finally, the authors thank the two referees whose constructive comments improved the present work.

[1] Z. Zakharov and V. E. Kuznetsov, "Three dimensional solitons," Sov. Phys. JETP **39**, 285–286 (1974).
[2] M. A. Allen and G. Rowlands, "Determination of the growth rate of the linearized Zkakarov Kuznetsov equation," J. Plasma Phys. **50**, 413–424 (1993).
[3] E. W. Laedke and K. H. Spatschek, "Limitations of two dimensional model equations for ion acoustic waves," Phys. Rev. Lett. **47**, 719–722 (1995).
[4] E. W. Laedke and K. H. Spatschek, "Growth rates of bending KdV solitons," J. Plasma Phys. **28**, 469–484 (1982).
[5] E. Infeld and P. Frycz, "Self-focusing of nonlinear ion acoustic waves and solitons in magetized plasmas Part 2. Numerical simulations, two soliton collisions," J. Plasma Phys. **37**, 97–106 (1987).
[6] R. M. Bradley, "Electromigration induced propagation on metal surfaces," Phys. Rev. E **60**, 3736–3740 (1999).
[7] R. M. Bradley, "Transverse instability of solitons propagating on current carrying metal thin films," Physica D **158**, 216–232 (2001).
[8] R. Sipcic and D. Benney, "Lump interactions and collapse in the modified Zakharov Kuznetsov equation," Stud. Appl. Math. **105**, 385–403 (2000).
[9] N. F. Smyth and A. L. Worthy, "Solitary wave evolution for mKdV equations," Wave Motion **21**, 263–275 (1995).
[10] A. A. Minzoni and N. F. Smyth, "Evolution of lump solutions for the KP equation," Wave Motion **24**, 291–305 (1996).
[11] W. L. Kath and N. F. Smyth, "Soliton evolution and radiation loss for the Korteweg-de Vries equation," Phys. Rev. E **51**, 661–670 (1995).
[12] G. B. Whitham, *Linear and Nonlinear Waves* (Wiley, New York, 1974).
[13] E. A. Kuznetsov, "Soliton stability in equations of the KdV type," Phys. Lett. **101A**, 314–316 (1984).
[14] E. A. Kuznetsov, A. M. Rubenchik, and V. E. Zakharov, "Soliton stability in plasmas and hydrodynamics," Phys. Rep. **142**, 103–165 (1986).
[15] E. A. Kuznetsov and V. E. Zakharov, *Nonlinear Coherent Phenomena in Continuous Media, Lecture Notes in Physics, Vol. 542, Nonlinear Science at the Dawn of the 21st Century*, edited by P. L. Christiansen, M. P. Soerensen, and A. C. Scott (Springer–Verlag, Berlin, 2000), pp. 3–45.
[16] G. Cruz-Pacheco, G. Flores-Reyna, M. C. Jorge, A. A. Minzoni, and N. F. Smyth, "Approximate evolution of lump initial conditions for the Benjamin-Ono equation," Wave Motion **28**, 195–202 (1998).
[17] B. Fornberg and G. B. Whitham, "A numerical and theoretical study of certain nonlinear wave phenomena," Philos. Trans. R. Soc. London, Ser. A **289**, 373–403 (1978).
[18] W. H. Press, S. A. Teukolsky, W. T. Vetterling, and B. P. Flannery, *Numerical Recipes in Fortran. The Art of Scientific Computing* (Cambridge U.P., Cambridge, 1992).